Atmospheric
Chemistry
and Physics
Discussions

Comparison of south Atlantic aerosol direct radiative effect over clouds from SCIAMACHY, POLDER and OMI/MODIS

Martin de Graaf[1], Ruben Schulte[2], Fanny Peers[3], Fabien Waquet[4], L. Gijsbert Tilstra[1], and Piet Stammes[1]

[1]Satellite Observations Department, Royal Netherlands Meteorological Institute (KNMI), De Bilt, The Netherlands
[2]Geosciences & Remote Sensing Department, Delft University of Technology (TUD), Delft, The Netherlands
[3]University of Exeter, Exeter, United Kingdom
[4]Université des Sciences et Technologies de Lille 1, Lille, France

Correspondence: Martin de Graaf (martin.de.graaf@knmi.nl)

Abstract. The Direct Radiative Effect (DRE) of aerosols above clouds has been found to be significant over the south-east Atlantic Ocean during the African biomass burning season due to elevated smoke layers absorbing radiation above the cloud deck. So far, global climate models have been unsuccessful in reproducing the high DRE values measured by various satellite instruments. Meanwhile, the radiative effects by aerosols have been identified as the largest source of uncertainty in global

5 climate models. In this paper, three independent satellite datasets of DRE during the biomass burning season in 2006 are compared to constrain the south-east Atlantic radiation budget. The DRE of aerosols above clouds is derived from the spectrometer SCIAMACHY, the polarimeter POLDER, and from collocated measurements by the spectrometer OMI and imager MODIS. All three confirm the high DRE values during the biomass season, underlining the relevance of local aerosol effects. Differences between the instruments can be attributed mainly to sampling issues. When these are accounted for, the remaining

10 differences can be completely explained by the higher cloud optical thickness derived from POLDER compared to the other instruments. Additionally, a neglect of AOT at SWIR wavelengths in the method used for SCIAMACHY and OMI/MODIS accounts for 26% of the difference between POLDER and OMI/MODIS DRE.

1 Introduction

15 Aerosol-cloud-radiation interactions currently present the largest uncertainty in our understanding of Earth's climate (Boucher et al., 2013). The effects of atmospheric aerosols are especially uncertain. Aerosols can absorb and scatter longwave and shortwave radiation, depending on their internal and external composition. These effects can be strongly amplified depending on the atmospheric composition. Clouds especially can alter the local radiation field, amplifying the aerosol effects and even changing the sign of the net effect.

20 Although many aerosol effects have been identified in model studies, constraining these models remains a challenge as observations of aerosol direct, indirect and semi-direct effects are scarce. The main problems are the complexities involved in

untangling the observations of aerosols, clouds and radiation in the real world. In this paper, we focus on the direct effect of aerosols above clouds, which can be characterized relatively well due to recent developments in retrieval techniques from a number of different satellite instruments.

The radiative effect of an atmospheric constituent can be defined as the net broadband irradiance change ΔF at a certain

5 level with and without the forcing constituent, after allowing for stratospheric temperatures to readjust to radiative equilibrium, but with tropospheric and surface temperatures and state held fixed at the unperturbed values (Forster et al., 2007). For tropospheric aerosols as the forcing agent, stratospheric adjustments have little effect on the radiative forcing and the instantaneous irradiance change at the Top Of the Atmosphere (TOA) can be substituted. The instantaneous aerosol Direct Radiative Effect (DRE) at TOA is therefore defined as the change in net (upwelling minus downwelling) irradiance, due to the introduction of

10 aerosols in the atmosphere. Since at TOA the downwelling irradiance $F^{\downarrow}$ is the incoming solar irradiance F_0 for all scenes, for a cloud scene the aerosol DRE can be determined from the difference between the upwelling irradiance in an aerosol-free cloud scene $F^{\uparrow}_{cld}$ and the upwelling irradiance of a scene with the same clouds plus aerosols $F^{\uparrow}_{cld+aer}$:

$$DRE_{aer} = (F^{\downarrow} - F^{\uparrow})_{cld} - (F^{\downarrow} - F^{\uparrow})_{cld+aer} = F^{\uparrow}_{cld+aer} - F^{\uparrow}_{cld}. \tag{1}$$

A radiative transfer model (RTM) is commonly used to, given the atmospheric constituents in the atmosphere, simulate the

15 scene twice; once with and once without the aerosols. To do this for a scene with aerosols overlying a cloud, the optical and physical properties of both the aerosols and the clouds have to be determined, and to a lesser extend the light absorption and scattering properties of the air and the surface reflectance.

The presence of clouds has a strong influence on the DRE from the light absorbing species in smoke at TOA. Over the dark ocean, in cloud-free scenes, scattering by the aerosols dominates and the planetary albedo is increased, resulting in a negative

20 direct effect (cooling). Over clouds, on the other hand, scattering by aerosols is negligible and the absorption dominates, lowering the planetary albedo, resulting in a positive direct effect (warming). E.g. an average change in forcing efficiency (DRE divided by AOT) from $-25\,\mathrm{Wm}^{-2}\tau^{-1}$ in cloud-free scenes to $+50\,\mathrm{Wm}^{-2}\tau^{-1}$ in fully clouded scenes was found by Chand et al. (2009). The DRE changed sign at a critical cloud fraction of about 0.4 for scenes over the south-east Atlantic Ocean. Similarly, simulations show that the DRE changed sign at a critical cloud optical thickness (COT) of about 4–8, a

25 higher COT resulting in a higher DRE (Feng and Christopher, 2015).

The south-east Atlantic has been a strong focus of modeling and observational studies of the aerosol DRE over clouds. The ocean west of the African continent, where sea surface temperatures are low due to upwelling of cold deep sea water, is covered by a semi-permanent cloud deck. During the austral winter months (July – October), which is the dry season on the adjacent African continent, a myriad of vegetation fires produces immense amounts of smoke (~ 25 Tg black carbon per year), resulting

30 in the largest source of black carbon and natural carbonaceous species in the atmosphere worldwide (van der Werf et al., 2010).

The combination of large areas of boundary layer clouds and overlying smoke proved to be a huge challenge for global climate models (GCMs) to simulate consistent aerosol DRE values at TOA. A comparison of sixteen GCMs showed a large range of aerosol DRE over the south-east Atlantic, from strongly negative (cooling) to strongly positive (warming) (Myhre et al.,

2013) for the same experiment, depending on the models' details on cloud and aerosol microphysical properties. It also shows that aerosol radiative effects can be very important on the local scale, near the source areas, whereas the contribution to the global radiative budget can be small.

Observations are needed to constrain the model simulations. This can be challenging, because ground observations are sparse and scarce, and satellite observations of COT and aerosol optical thickness (AOT) are difficult to disentangle. COT observations in the common visible region are biased by absorption by aerosols, resulting in a biased DRE estimation (Haywood et al., 2004; Coddington et al., 2010). Satellite AOT retrievals are commonly performed only in cloud-free scenes, hampering the computation of the aerosol DRE in cloud scenes.

One way of separating cloud and aerosol scattering is the use of active (lidar) instruments, which produce vertically high resolution backscatter profiles, e.g. CALIOP onboard CALIPSO (Chand et al., 2009; Meyer et al., 2013; Zhang et al., 2014). Unfortunately, the spatial coverage of a lidar is limited. Another solution is the use of polarimeter measurements. The different effects of spherical water droplets and irregularly shaped aerosol particles on the polarisation of light can be used to separate the cloud and aerosol contribution to the radiation at TOA. This was applied to POLDER measurements (Waquet et al., 2013a). The absorption from the aerosol layer and the COT is retrieved using reflectances measured in the visible and shortwave infrared. Finally, the aerosol DRE in cloud scenes can be computed using an RTM. The instantaneous DRE values from POLDER for aerosols over clouds over the south-east Atlantic in 2006 have been the highest yet, up to $125\,\mathrm{Wm^{-2}}$ (Peers et al., 2015).

The absorption by small smoke aerosols is especially strong in the UV. Several methods use this principle to separate the cloud scattering from the aerosol absorption and scattering. The strong UV absorption can be quantified by the UV Aerosol Index (UV-AI) (de Graaf et al., 2005, 2007; Wilcox, 2012), while the reduction in reflectance in the UV and visible channels can be simulated using LookUp Tables (LUTs). This was used to retrieve AOT of smoke above clouds in the south-east Atlantic, and the COT of the clouds underneath simultaneously, using OMI measurements (Torres et al., 2011). A similar method was applied to MODIS measurements to retrieve AOT and COT simultaneously, using measurements in the visible (Jethva et al., 2013).

These methods all rely on the quantification of the optical properties of the aerosols. However, light absorption by smoke is highly variable and the spectral dependence (quantified by the Ångtröm parameter) is much larger than often assumed (Jethva and Torres, 2011) and not necessarily unique (Bergstrom et al., 2007). The AOT over clouds in the south-east Atlantic derived from POLDER, CALIOP and MODIS measurements were compared in Jethva et al. (2014), showing a general agreement, but large differences in the details.

Spectral information of the aerosol and cloud properties is needed to correctly specify the aerosol-cloud-radiation interactions at all wavelengths. Measurements from six wavelength channels from MODIS (from 0.47–1.24μm) have been used to retrieve COT and cloud droplet effective radius (CER) for clouds with overlying aerosols, simultaneously with the above–cloud AOT, and subsequently aerosol DRE (Meyer et al., 2015). However, here also the aerosol spectral properties have to be assumed. To circumvent the use of aerosol optical property models altogether, the spectral dependence of aerosol absorption can be measured with hyperspectral satellite instruments like SCIAMACHY (de Graaf et al., 2012). The principle here is that the absorption by the aerosols is captured entirely by the radiance measurements in the UV, visible and SWIR regions, and only

the aerosol-free atmosphere is simulated in an RTM. The cloud properties can be retrieved in the SWIR where small particles like smoke have little to no effect on the COT and CER. The DRE is then retrieved from a difference in simulated and measured reflectance, and the difference is attributed to absorption by aerosols. Hence it is termed differential aerosol absorption (DAA) method. The DRE retrieved in this way from SCIAMACHY was compared to Hadley Centre Global Environmental Model

5 version 2 (HadGEM2) climate model simulations, showing that even this GCM, which simulated a large warming over the south-east Atlantic, still fell short in simulating the UV-absorption by smoke (de Graaf et al., 2014). The DAA method was recently applied to a combination of OMI and MODIS reflectance measurements (de Graaf et al., 2019).

The main challenge in comparing satellite data is the wide range in spatial resolution and sampling of different instruments. To resolve this, many papers report area- and time-averaged DRE values and compare them to other average values of the

10 aerosol DRE. In this paper, the DRE derived from POLDER measurements are compared to the DRE from SCIAMACHY and to DRE derived from a combination of OMI and MODIS measurements, accounting explicitly for sampling issues. While POLDER reports consistently high values of AOT, COT and DRE compared to other instruments, we show that the DRE values agree to within the error estimates when sampling issues are accounted for, except for the extreme high values.

2   Methods

15 ### 2.1   POLDER DRE

POLDER is a passive optical imaging radiometer and polarimeter on-board the Polarization and Anisotropy of Reflectances for Atmospheric Science coupled with Observations from a Lidar (PARASOL). PARASOL was launched in December 2004 and was part of the A-Train satellite constellation for five years. After 2009, PARASOL's orbit was lowered, and it fully exited the A-Train in 2013. POLDER provides radiances in nine spectral bands between 443 and 1020 nm and polarisation

20 measurements at 490, 670 and 865 nm. The ground spatial resolution is about $5.3 \times 6.2 \, \text{km}^2$ and the swath width about 1100 km (Deschamps et al., 1994). All measurements of POLDER are projected on a fixed global reference grid of $6 \times 6 \, \text{km}^2$.

The POLDER method retrieves the above-cloud AOT, the aerosol Single Scattering Albedo (SSA) and the COT in two steps. The first one consists of using the polarization radiance measurements to retrieve the scattering AOT and the aerosol size distribution in a cloudy scene. Aerosols affect the polarisation in a cloudy scene in two ways. Firstly, the large peak of

25 the signal around a scattering angle of $140°$, caused by the liquid cloud droplets, is attenuated. Secondly, an additional signal at side scattering angles is created. The effect of absorption is assumed to be very weak at these angles and mostly treated as a scattering process. In the second step, the spectral contrast and the magnitude of the total radiances measured in the visible and SWIR are used to retrieve the absorption AOT and COT simultaneously. Therefore, the retrieval of the aerosol properties is done with minimal assumptions and with the cloud properties corrected for the overlying aerosol absorption. To ensure the

30 quality of the products, several filters are applied, which include the removal of inhomogeneous clouds, broken clouds, cloud edges, clouds with COT lower than 3 and cirrus (Waquet et al., 2013b; Peers et al., 2015).

The POLDER DRE is finally calculated over the south-east Atlantic for aerosols over clouds in 2006 using the retrieved AOT, SSA and COT with the method described in section 3 of Peers et al. (2015). POLDER apparent O_2 cloud top pressures

were used to constrain the cloud layer height, although the cloud top pressure has been shown to have a negligible effect on the TOA radiation (less than 1% for a change of 200 hPa (Ahmad et al., 2004; de Graaf et al., 2012)). CER was derived from collocated MODIS measurements. The DRE was derived for all scenes with a geometric cloud fraction (CF) of 1.0 and a COT larger than 3.0. The surface reflectance was computed taking surface winds (from models) into account (Cox and Munk, 1954),

5 but since only scenes with a minimum COT of 3 were used, the influence of the surface reflectance on the total radiation field will be small. The ozone and the water vapour content were obtained from meteorological reanalysis.

2.2 SCIAMACHY DRE

The DAA method was developed for reflectance spectra from the SCanning Imaging Absorption spectroMeter for Atmospheric CHartographY (SCIAMACHY). SCIAMACHY was part of the payload of the Environment Satellite (EnviSat), launched in

10 2002, into a polar orbit with an equator crossing time of 10:00 LT for the descending node, but stopped delivering data in 2012. SCIAMACHY observed radiation in two alternating modes, nadir and limb, yielding data blocks called states, approximately $960{\times}490\,\mathrm{km}^2$ in size. In nadir mode, SCIAMACHY measured continuous reflectance spectra from 240–2380 nm with a spatial resolution of about $60{\times}30\,\mathrm{km}^2$ and a spectral resolution of 0.2–1.5 nm (Bovensmann et al., 1999). This unique spectral range from the UV to the shortwave infrared (SWIR) contains 92% of the incoming solar irradiance. The DRE was determined from

15 SCIAMACHY reflectance spectra of cloud scenes in 2006 over the south-east Atlantic. Cloud properties were determined at 1.2 and 1.6 μm, where absorption by smoke is assumed to be negligible. Effective CF and cloud pressure (CP) were determined from FRESCO (Wang et al., 2008). All scenes with effective CF > 0.3, CP > 850 hPa and COT > 3.0 were used to select pixels with sufficient water clouds only. Total ozone was accounted for, but this has a negligible impact on the DRE.

2.3 DRE from combined OMI-MODIS reflectances

20 The absorption of radiation by aerosols is spectrally dependent, but since the particles vary in size and composition, the spectral dependence is smooth, as opposed to absorption by (trace) gases, which is strongly peaked in absorption lines. Therefore, the DRE data record from SCIAMACHY was continued using a combination of spectrally high-resolution OMI reflectances and low-resolution MODIS reflectances, which are sufficient to capture the spectral dependence of the absorption in the visible and SWIR.

25 OMI (Levelt et al., 2006), on-board the Aura satellite, was launched in 2004, to measure the complete spectrum from the UV to the visible wavelength range (up to 500 nm) with a high spatial resolution, similar to SCIAMACHY. The Earth shine radiance is observed in a swath width of about 2600 km, covering almost the entire Earth in one day. The spatial resolution of OMI is typically about $15{\times}23.5\,\mathrm{km}^2$ at nadir to about $42{\times}126\,\mathrm{km}^2$ for far off-nadir (56 degrees) pixels. Since 2008, OMI suffers from progressive degradation, especially in far off-nadir pixels, called the row anomaly.

30 MODIS, on-board the Aqua satellite, flies in formation with Aqua in the A-Train, leading Aqua by about 15 minutes (in 2006, while PARASOL was placed in between these two instruments). MODIS measures radiances in broad bands (typical about 20–50 nm) from the visible to SWIR, with a typical spatial resolution of 250–500 m. Spectrally, OMI overlaps with MODIS at 459–479 nm (central wavelength 469 nm), which can be used to match the OMI reflectances in the visible channel

Table 1. Maximum and average values of OMI/MODIS, SCIAMACHY, and POLDER DRE on 12 and 19 August 2006 for the areas shown in Figures 1(d–f) and 1(a–c).

12 August 2006	Max DRE	$\langle$DRE$\rangle$
POLDER	303.8	109.1
OMI/MODIS	120.0	35.5
SCIAMACHY	112.5	28.4
19 August 2006		
POLDER	190.3	43.0
OMI/MODIS	94.0	11.4
SCIAMACHY	71.3	18.1

and the MODIS reflectance in band 3 (de Graaf et al., 2016). This way, a continuous low-resolution spectrum at OMI resolution is available to which DAA can be applied (de Graaf et al., 2019).

The DRE was determined from OMI pixels over the south-east Atlantic in 2006. COT and CER were determined at 1.2 and 2.1 μm, because of a reduced sampling in MODIS/Aqua 1.6 μm band due to nonfunctional detectors (Meyer et al., 2015). CP and effective CF are available from OMI O_2-O_2 retrievals. All scenes with COT > 3.0, effective CF > 0.3 and CP > 850 hPa were selected.

2.4 Error budget

The largest uncertainty in the DAA method derives from the assumption that the aerosol-free cloud scene can be simulated using an RTM, which is assumed in all methods. For SCIAMACHY and OMI/MODIS scenes this was actually tested, by applying the technique to measured aerosol-free cloud scenes and determining the DRE, which should be zero by definition. This provides an easy verification of the method. For each instrument and area this can be determined separately, by screening cloud scenes with overlying absorbing aerosol using the aerosol UV index, which is highly sensitive to UV-absorbing aerosols. The (average) deviation of the DRE from zero, determined for aerosol-free cloud scenes, is a good estimate of the uncertainty of the method, which can be substantial. Note however, that such an estimate is often missing, while methods other than DAA are moreover highly uncertain due to their dependence on the correct characterization of the spectral properties of the overlying aerosols. Other minor error sources for the DAA method are the uncertainty in input parameters, the influence of the smoke on the estimated cloud fraction, cloud optical thickness and cloud droplet effective radius, an uncertainty in the anisotropy factor (de Graaf et al., 2019), and the uncertainty of estimating the COT and CER at SWIR wavelengths. The error on the aerosol DRE from SCIAMACHY is about 8 Wm^{-2} (de Graaf et al., 2012) and from OMI/MODIS about 13 Wm^{-2} (de Graaf et al., 2019).

3 Results

3.1 Case studies in August 2006

The aerosol DRE retrievals over clouds from the various satellite instruments are illustrated in Figure 1 for two cases in August 2006. August is the peak of the biomass burning season in southern Africa, and an extended smoke plume, originating from the

5   African continent, drifted over the south-east Atlantic Ocean in an elevated layer above a stratocumulus deck in the boundary layer. The absorption of radiation by the smoke above the stratocumulus cloud deck is indicated by high DRE values, in cloud scenes only. On the left the situation on 19 August 2006 is given, which shows a good correlation between the instruments. Figure 1a shows the POLDER DRE overlaid an a MODIS RGB image acquired around 13:20 UTC, Figure 1b the OMI/MODIS DRE over the same MODIS RGB image, and Figure 1c the SCIAMACHY DRE overlaid over a MERIS RGB image, both

10   on EnviSat. Envisat is in a morning orbit, and the SCIAMACHY and MERIS measurements were taken around 9:30 UTC. Clearly, the clouds are more extensive in the latter image, because clouds in this area break up as the day progresses and the solar radiation intensifies (Bergman and Salby, 1996).

Obviously, the spatial coverage of SCIAMACHY is much lower than OMI and MODIS, measuring in nadir mode only half of the time, and having larger pixels. Consequently, the OMI/MODIS DRE is smoother with a better coverage. However, the

15   most striking feature is the much higher values from POLDER compared to the other two instruments, even though the general DRE patterns for the three instruments are quite similar. The POLDER DRE reaches values up to 190 Wm^{-2} in parts where smoke from the African continent is abundant. The values drop off to zero over clouds where the smoke plume is thinning. The DRE from the two other instruments, on the other hand, is never larger than 100 Wm^{-2}. The DRE values for these cases are summarized in Table 1

20   On the right, the figure shows the situation for 12 August 2006, when the comparison between the instrument is worst. Figures 1d–f show the same data as Figures 1a–c, only one week earlier and from a slightly different area, centered on the MERIS and SCIAMACHY overpass.

Obviously, there are clear differences between the retrievals. The POLDER DRE is very large, reaching values up to 304 Wm^{-2}. The OMI/MODIS DRE is larger than on 19 August 2006, reaching up to 120 Wm^{-2}, but still much lower than the

25   POLDER DRE. The SCIAMACHY DRE shows similar values and patterns as OMI/MODIS DRE, but the coverage is rather poor. The maximum SCIAMACHY DRE was 113 Wm^{-2}. The differences between the datasets will be explained below by a closer inspection of the data and the retrievals.

3.2 Area-averaged DRE

When comparing datasets, and datasets and simulations, sampling is a serious issue. Often, area- and time-averages are com-

30   pared, to reduce the effects of sampling differences. Here, we show the effect of ignoring the sampling effect, even of area-averages of, in this case, aerosol DRE over clouds.

In Figure 2a, the area-averaged instantaneous aerosol DRE over clouds from all three instruments is given for all available data in the area 10°N–20°S,10°W–20°E, between 1 June and 1 October 2006. This is the biomass burning season and the area

where often area-averaged DRE values have been reported during this season (e.g. Chand et al., 2009; de Graaf et al., 2014; Meyer et al., 2013; Peers et al., 2015). Since the instruments have different overpass times, the instantaneous aerosol DRE over clouds was normalized by dividing by the cosine of the solar zenith angle. Therefore, the quantity in Figure 2a represents the instantaneous aerosol DRE at noon, which is generally higher than the instantaneous aerosol DRE measured during the overpass. Figure 2a shows the evolution of the biomass burning season in 2006, with low DRE values in June, high values in July, extreme values in August and moderate values in September.

The area-averaged DRE of smoke over clouds reaches values up to 100 Wm^{-2} and more in mid-August 2006, according to SCIAMACHY and POLDER. The events during this period have been investigated often before (e.g. Chand et al., 2008; Jethva and Torres, 2011; Yu and Zhang, 2013). The SCIAMACHY DRE values were compared to model calculations from GCMs, particularly HadGEM2 (de Graaf et al., 2014). Models were not able to replicate these extremely high aerosol direct radiative effects. The emission of smoke from Africa was possibly strongly peaked in August, but even accounting for such episodic emissions in models did not explain the difference in aerosol effects in models and observations by SCIAMACHY. And Figure 2a shows that the aerosol DRE values from POLDER are even higher than those from SCIAMACHY. On the other hand, the average OMI/MODIS DRE is never higher than about 60 Wm^{-2}. The largest difference between the datasets was found on 12 August 2006.

The differences between the instruments are illustrated using histograms of all noon-normalized aerosol DREs, see Figure 3a. Clearly, the average POLDER aerosol DRE is almost twice as large as that from OMI/MODIS and SCIAMACHY (24.9 Wm^{-2} for OMI/MODIS, 28.4 Wm^{-2} for SCIAMACHY and 46.6 Wm^{-2} for POLDER). The statistics of the distributions are given in Table 2. In only the month August, the average aerosol DRE was 27.5 Wm^{-2} for OMI/MODIS, 36.8 Wm^{-2} for SCIAMACHY and 49.7 Wm^{-2} for POLDER. This is a somewhat larger difference between POLDER and SCIAMACHY than found by Peers et al. (2015) (about 10.5 Wm^{-2} difference between SCIAMACHY and POLDER), but there POLDER DRE was averaged over a much larger area containing more small values of DRE.

The histograms show that the DRE from POLDER is higher than the DRE from OMI/MODIS mainly due to more large DRE values. This is indicated by the larger positive skewness for POLDER, a measure for the asymmetry of the distribution, where the other instruments show a more symmetric distribution.

The main reason for the much larger area-averaged POLDER DRE on 12 August 2006 is the smaller coverage of the area by POLDER, compared to that by OMI/MODIS, due to a smaller swath. This was illustrated in Figures 1d and 1e. In 1d the entire left part of the image is not sampled. In this case, this results in a sampling by POLDER of only the very high DRE values that are found near the continent, while OMI and MODIS sample the entire basin, which has large parts with very low to zero aerosol DRE. In the case of SCIAMACHY only about 1/6 of the area is covered by SCIAMACHY nadir measurements, which obviously makes it very sensitive to the sampling of an aerosol plume during one overpass. OMI and MODIS have a much better coverage, sampling most of the area during an overpass.

However, OMI pixel sizes vary between nadir and the far off-nadir pixels by a factor of 15. This means that a (dense) plume may be sampled once by a far off-center pixel, or by 15 nadir pixels, all of them receiving the same high values, depending on the satellite track. The pixel sizes of SCIAMACHY are even larger. The POLDER pixels sizes, on the other hand, are constant

Atmospheric
Chemistry
and Physics
Discussions

Table 2. DRE Statistics of the different instruments before and after collocation for the area $10°$N–$20°$S;$10°$W–$20°$E in the south-east Atlantic.

Native grid	Mean	Median	Std. Dev	Skewness
POLDER	46.60	38.74	39.00	1.57
OMI/MODIS	24.88	21.92	30.27	0.62
SCIAMACHY	28.42	26.11	24.62	1.26
Collocated				
POLDER	46.96	37.88	41.01	1.83
OMI/MODIS	34.50	31.48	27.69	1.41
SCIAMACHY	39.47	36.23	24.68	1.25

on a relatively fine $6{\times}6$ km^2 grid. The different pixel sizes produce a difference in the extreme values. Due to the larger pixel sizes, small features in OMI/MODIS and SCIAMACHY will be more smoothed out compared to POLDER data.

Additionally, on 12 August 2006 at some places where the highest values of aerosol DRE can be expected, the OMI/MODIS retrievals failed (Figure 1d), probably due to broken cloud scenes in combination with very high aerosol loadings, which resulted in low scene reflectances which were not marked as clouded scenes. Furthermore, cloud filtering can be different for the three instruments, due to the use of different cloud filters (use of effective or geometrical cloud fractions), which may have a strong influence on the (average) DRE.

3.2.1 Sampling

Clearly, these different spatial scales limit the usefullness of a comparison of average values from satellite instruments. In order to correct for the issues described above, the OMI/MODIS and SCIAMACHY measurements were regridded onto a regular lat/lon grid, of $6666{\times}3333$ grid points. This corresponds to a 6 km $\times$ 6 km grid at the equator (reducing to $5.6{\times}5.6$ km^2 at $20°$S). All regular grid cells covered by a SCIAMACHY or OMI pixel were given the value of that SCIAMACHY or OMI/MODIS DRE measurement. This gave SCIAMACHY and OMI/MODIS DRE values on a grid similar to the POLDER grid (albeit smoothed per OMI or SCIAMACHY pixel), so that values can be compared on a pixel-per-pixel basis. The individual POLDER DRE values were then compared to the OMI/MODIS and SCIAMACHY DRE values in the grid cell that was closest to the POLDER grid cell. In Figure 2b the area-averaged instantaneous DRE over clouds over the south-east Atlantic is shown, like in Figure 2a, but using only those pixels that are covered by all three instruments. This effectively removes all sampling issues and differences due to different cloud screening strategies for the instruments. Note that at a number of days no values were available, since there were simply no areas with DRE that are sampled by all three instruments! This underlines the importance of sampling, even for such a fairly large area. The number of pixels over which was averaged per day is shown in the lower panel of Figure 2b.

The correlation between the noon-normalised area-averaged instantaneous DRE from the three instruments is now significantly improved compared to Figure 2a. The aerosol DRE from OMI/MODIS follows the aerosol DRE from SCIAMACHY

very closely for almost the entire period shown. Note that the maximum DRE from OMI/MODIS is now increased to almost $100 \, \mathrm{Wm}^{-2}$, which was due to removing many pixels with a moderate to low DRE during mid-August, that were not covered by POLDER and SCIAMACHY, as illustrated in Figures 1d–f. The difference in average DRE between the instruments is also greatly reduced, see Figure 3b, which shows the histograms for only overlapping regridded pixels. The average DRE from

5   POLDER is still about $47.0 \, \mathrm{Wm}^{-2}$ for only overlapping pixels, while the average DRE from OMI/MODIS has increased to $34.5 \, \mathrm{Wm}^{-2}$ and $39.5 \, \mathrm{Wm}^{-2}$ for SCIAMACHY regridded pixels.

The skewness of the OMI/MODIS DRE distribution is now closer to the skewness of the distribution of POLDER DRE, but still the POLDER distribution is dominated by high values. This is also clear from a scatterplot of POLDER DRE vs. OMI/MODIS DRE for regridded OMI/MODIS pixels, shown in Figure 4a. Note that for this plot only a POLDER and

10   OMI/MODIS overlap was required, which yielded a significantly higher number of pixels than when also SCIAMACHY overlap was required. The figure shows a good correlation of aerosol DRE for most measurements, but at high values of the DRE, the OMI/MODIS DRE is systematically underestimated compared to POLDER DRE. The average ratio of OMI/MODIS DRE to POLDER DRE is 0.82, while a normal linear least-squares fit (shown by the green line in Figure 4a) yields a slope of OMI/MODIS to POLDER ratio of only 0.56. This is because the fit is dominated by the large values, while the large majority

15   of points are moderate values around $25 \, \mathrm{Wm}^{-2}$. When a fit is drawn which is weighted to the majority of the points (shown by the red line), a slope of 0.74 is found, which is closer to the average ratio.

SCIAMACHY DRE is very similar to OMI/MODIS DRE for all pixels sampled by these instruments (not shown).

Several reasons for the smaller SCIAMACHY and OMI/MODIS DRE compared to POLDER DRE exist. First, a sampling issue still remains, since the regular grid cells contain DRE values from larger OMI and SCIAMACHY pixels. Therefore, the

20   high resolution grid cells receive smoothed values. This issue could be resolved if all values were regridded to the coarsest available. However, since this is the SCIAMACHY grid, not many grid cells would remain.

3.2.2   AOT differences

Another explanation is an underestimation of the AOT by SCIAMACHY and OMI/MODIS and a possibly overestimation of the AOT by POLDER. The POLDER DRE is dependent on the retrieved AOT and COT, which in principle are both unbounded.

25   When the algorithm retrieves very large values for both, the derived DRE can also become very large. In mid-August, DRE above $300 \, \mathrm{Wm}^{-2}$ were often reached, up to more than $400 \, \mathrm{Wm}^{-2}$ for the SZA-corrected DRE. This is 30% of the maximum incoming solar irradiance. The POLDER AOT at 550 nm on 12 August 2006 was 1.1, averaged over the entire area, with individual values up to 1.9, which is extremely high. However, high AOT for this plume was found before. Chand et al. (2009) found an AOT of up to 1.5 (532 nm) using CALIOP data, Jethva et al. (2013) found above-cloud AOT observed from MODIS

30   up to 2.0 for this day. A comparison between AOT above clouds from several instruments (Jethva et al., 2014) showed POLDER to be on the high side, but not necessarily strongly overestimated. Comparisons with CALIOP observations revealed that the CALIOP above-cloud AOT from the operational retrieval are underestimated, while the above-cloud AOT from POLDER and the CALIOP depolarisation ratio method are well-correlated (Deaconu et al., 2017).

When aerosols are mixed into the cloud layer the polarization signal may be enhanced, and POLDER AOT may possibly be high-biased. Also, when the smoke has a high real refractive index ($m_r > 1.47$) the AOT is overestimated by POLDER (Peers et al., 2015). However, it has been shown that the real part of the refractive index has mostly an impact on the scattering AOT. In the case of biomass burning aerosols above clouds, the absorption AOT, which is retrieved by POLDER with a better

5 accuracy, has a larger influence on the DRE calculation.

The DRE from SCIAMACHY and OMI/MODIS is limited to about 200–250 Wm^{-2} for individual pixels. Since the DRE for these instruments is determined by assuming an AOT of zero at 1.2 μm and calculated as a fraction of the incoming local irradiance, it is unlikely to reach extremely high values. This assumption of negligible AOT at longer wavelengths is valid for sufficiently small particles, but may break apart at very high AOT, or for larger particles. The AOT at 1.2 μm may be estimated

10 from the POLDER 550 nm AOT, using an Ångström parameter of 1.45, which was found in the spectral region from 325 to 1000 nm for African biomass burning aerosols from SAFARI 2000 observations (Bergstrom et al., 2007; Russell et al., 2010). This way, an AOT at 1.2 μm can be found between 0.15 and 0.35 during the smoke peak in mid-August 2006, occasionally even reaching 0.6 (Schulte, 2016). The effect on DRE of neglecting a non-zero AOT at 1.2 μm in DAA was estimated at 21.7 Wm$^{-1}\tau^{-1}$ (de Graaf et al., 2012), so these AOTs given by POLDER would result in an underestimation of the DRE by

15 both SCIAMACHY and OMI/MODIS of up to 13 Wm^{-2}. This would explain about 26% of the difference of up to 50 Wm^{-2} between the DRE from POLDER and SCIAMACHY or OMI/MODIS shown in Figure 2.

3.2.3   COT differences

The DRE depends more strongly on the COT of the cloud underlying the smoke than the AOT of the smoke. A comparison of SCIAMACHY, OMI/MODIS and POLDER COT histograms (not shown) revealed a slightly higher COT from SCIAMACHY

20 and OMI/MODIS compared to POLDER (up to 42 for POLDER and 48 for OMI/MODIS (Schulte, 2016)), but the maximum of POLDER is restricted due to LUT limits. Note that POLDER COT is retrieved at 0.87 microns, while COT from OMI/MODIS and SCIAMACHY is retrieved at 1.2 microns. However, the spectral variation in COT is very small. Only for very small cloud droplets the COT at 0.87 microns is about 4% smaller than the COT at 1.2 microns for cloud droplet effective radii of 4 microns, and this reduces for larger droplets. For SCIAMACHY, the COT may also be different because of its morning overpass, when

25 the cloud cover is systematically thicker than in the afternoon. In Figure 5, the COT from POLDER is compared to the COT derived from OMI/MODIS on 19 August 2006, regridded to a 6x6 km^2 regular grid. It shows that the high DRE values in Figure 1 are highly correlated with high COT values (which makes sense, since the AOT varies rather smoothly over the area). However, it also shows that the POLDER COT peaks are much larger than those from OMI/MODIS. Even though the OMI/MODIS data are regridded to a high resolution grid, the values are obviously still more smoothed compared to the COT

30 on the native high resolution POLDER grid. Therefore, even though POLDER COT and POLDER DRE are generally smaller than from OMI/MODIS on average, the extreme values and averages are higher.

To illustrate the effect of a higher COT on the DRE retrieval, the average COT from both POLDER and OMI/MODIS on the case studies for collocated pixels were compared. Then, the above-cloud DRE have been calculated for OMI/MODIS and POLDER using their mean COT and the mean AOT retrieved by POLDER. Results are summarized in Table 3. On 19

Table 3. Average values of the OMI/MODIS COT and the POLDER COT and above-cloud AOT on 12 and 19 August 2006 between 20–0°S;8°W–14°E. The DRE was calculated at noon using the average AOT and COT, assuming a cloud droplet effective radius of 8 μm, an aerosol SSA of 0.840 at 550 nm and an aerosol geometric radius of 0.1μm.

	Max COT	$\langle$COT$\rangle$	$\langle$AOT$\rangle$	$\langle$DRE$\rangle$
			POLDER	Wm^{-2}
12 August 2006				
POLDER	42.0	14.8	1.25	184.1
OMI/MODIS	24.1	10.1	*1.25*	134.3
19 August 2006				
POLDER	42.0	11.8	0.578	83.3
OMI/MODIS	47.7	9.4	*0.578*	66.9

August 2006, the mean COT from OMI/MODIS was 9.4 (max. 48), while from POLDER the mean COT was 11.8 (max. of 42). Based on a mean AOT of 0.578, an aerosol DRE over clouds of 83 Wm^{-2} and 67 Wm^{-2} have been obtained from the average COT from POLDER and OMI/MODIS, respectively. On 12 August 2006, the average COT from POLDER was 14.8, and from OMI/MODIS 10.1, while the average POLDER AOT was 1.25. This results in a DRE of 184 Wm^{-2} for POLDER

5 and 134 Wm^{-2} for OMI/MODIS. This suggest that the COT difference can completely account for the difference of up to 50 Wm^{-2} between the DRE from POLDER and SCIAMACHY or OMI/MODIS shown in Figure 2.

To show the effect of the COT on the DRE retrieval, in Figure 4b the DRE divided by the COT is shown for OMI/MODIS vs. POLDER. It shows that the difference between these two quantities disappears completely for these instruments, and the slope is even reversed. Clearly, the COT has the largest impact on the computation of the aerosol DRE over clouds. Since the

10 POLDER instrument retrieves higher values of COT in smaller pixels, the DRE is subsequently higher.

The errors in AOT and COT are not independent. In the DAA method, when the assumption of negligible AOT at longer wavelengths is no longer valid (large concentration of aerosols and/or large particles), the estimated COT is biased, resulting in a bias in the DRE. A better estimate of the DRE from the DAA method could be obtained when an unbiased retrieval of the COT was used, like e.g. from POLDER.

15 **4 Conclusions**

In this paper, the aerosol direct radiative effect product is presented for cloud scenes in the south-east Atlantic, retrieved from SCIAMACHY reflectances, combined reflectance measurements from OMI and MODIS, and POLDER COT and AOT measurements in 2006. During this year, the production of smoke from vegetation fires in Africa was very large, and all instruments performed well. The average DRE from SCIAMACHY and OMI/MODIS, both retrieved using DAA, correspond

20 very well, even though OMI/MODIS DRE has a much better resolution and coverage. The aerosol DRE from POLDER is completely independent. It correlates well with SCIAMACHY and OMI/MODIS DRE for moderate values, but is larger than

SCIAMACHY and OMI/MODIS DRE for high values. This is caused by a larger COT retrieved by POLDER, and to a lesser degree by an underestimation of the aerosol DRE using DAA, which by definition assumes a zero AOT at SWIR wavelengths.

The largest contribution to the difference between SCIAMACHY, OMI/MODIS and POLDER DRE are sampling issues. Regridding SCIAMACHY and MODIS/OMI to the native POLDER grid and selecting only pixels sampled by all three instru-

5   ments improved the comparison considerably. This approach removes issues related to selecting high positive DRE values by filtering on COT and CF, which introduce large differences in the average DRE. Only smoothing due to the large footprints of SCIAMACHY and OMI remains, which is reflected in the less extreme COT and DRE values compared to POLDER.

After removing sampling issues, the largest remaining differences in DRE are caused by different estimates of the COT using the various instruments. Since the bright background of clouds determines the measured reflectance to a very large degree, the

10 DRE is strongly dependent on the COT. COT can change on small spatial scales. This is reflected in the higher positive skewness of the POLDER DRE. The POLDER DRE distribution is less symmetric with larger tails than those from SCIAMACHY and OMI/MODIS, due to the high spatial resolution of the POLDER measurements. The POLDER COT is systematically higher than that from OMI/MODIS and SCIAMACHY. Normally, MODIS COT retrievals at 0.8 and 1.2 microns retrievals are very close to POLDER COT for fully clouded scenes with liquid water clouds (Zeng et al., 2012) (not considering overlying smoke).

15 However, to avoid biases from smoke absorption, the MODIS channels at 1.2 and 2.1 microns are used to derive COT and CER for OMI/MODIS DRE retrievals. In our retrievals the MODIS reflectances at a resolution of $1° \times 1°$ are first aggregated to the OMI spatial grid, and for this analysis regridded back to the POLDER grid. This will smooth extreme values. When the DRE was divided by the retrieved COT, the difference between the instruments is reversed, OMI/MODIS DRE/COT being larger than POLDER DRE/COT. This shows that a correct COT is essential for the determination of the direct radiative effect of

20 aerosols above clouds. The difference in average COT from OMI/MODIS and POLDER can explain 100% of the difference in DRE on 12 August 2006.

The AOT is assumed to be zero at 1.2 microns in DAA, but was estimated from POLDER to be up to 0.6 in extreme cases, which resulted in an underestimation of the DRE in DAA of 13 Wm^{-2}. Comparing AOT over clouds POLDER with MODIS and CALIOP, showed POLDER to be high, but not necessarily overestimated. The underestimation of the AOT for high values

25 can explain about 26% of the difference in DRE between POLDER and OMI/MODIS om 12 August 2006.

This analysis shows that the aerosol direct effect of aerosols above clouds can be significant on the local scale when smoke is present over clouds. So far, model simulations have been unable to reproduce the high values, and many models underestimate the signal and even simulate a cooling (Myhre et al., 2013), where the datasets in this analysis clearly show that the positive effect is significant and real. However, when observations and model simulations of local effects are compared, sampling issues

30 should be properly accounted for, because area-averaging and time-averaging does not work well for episodic events like smoke plumes, which are short-lived and localized.

The analysis also shows the strengths and weaknesses of the DRE retrieval algorithms for POLDER, SCIAMACHY and OMI/MODIS. Clearly, the latter two still suffer from a bias in the cloud parameter retrieval when smoke is abundant, providing a lower limit of the aerosol DRE over clouds. POLDER DRE takes advantage of the polarization measurements to accurately

35 estimate the COT, CER and AOT, without interdependent biases. However, for the spectral dependence of the aerosol absorp-

Atmospheric
Chemistry
and Physics
Discussions

tion in the UV, there is still a dependence on the choice of aerosol model. A combination of the two methods, DAA and DRE based on polarization measurements, could provide very accurate measurements of aerosol DRE over clouds, which is feasible for upcoming missions like METOP-SG 3MI (Marbach et al., 2015). This mission combines spectral imaging and polarization measurements. The DAA method would benefit from unbiased COT retrievals, that could be provided with polarization

5 measurements. The assumptions on the spectral dependence of the aerosol absorption in the POLDER-like retrieval can be assessed and improved by the DAA method in a closure study using the instruments on the METOP-SG 3MI platform. This would allow time-dependent retrievals of UV-absorption by aerosols above clouds.

The POLDER, SCIAMACHY and OMI/MODIS DRE products provide datasets that can be used to challenge GCMs and test their aerosol intrinsic properties and aerosol-cloud-radiation interaction schemes.

10 *Data availability.* The data used in this study is available from the authors.

Author contributions. MdG, LGT and PS are responsible for the DRE datasets from SCIAMACHY and OMI/MODIS. FP and FW are responsible for the POLDER dataset. RS initially compared the datasets.

Competing interests. The authors declare no competing interests.

Atmospheric
Chemistry
and Physics
Discussions

References

Ahmad, Z., Bhartia, P. K., and Krotkov, N.: Spectral properties of backscattered UV radiation in cloudy atmospheres, J. Geophys. Res., 109, D01201, https://doi.org/10.1029/2003JD003395, 2004.

Bergman, J. W. and Salby, M. L.: Diurnal Variations of Cloud Cover and Their Relationship to Climatological Conditions, J. Climate, 9, 2802–2820, https://doi.org/10.1175/1520-0442(1996)009<2802:DVOCCA>2.0.CO;2, 1996.

Bergstrom, R. W., Pilewskie, P., Russell, P. B., Redemann, J., Bond, T. C., Quinn, P. K., and Sierau, B.: Spectral absorption properties of atmospheric aerosols, Atmos. Chem. Phys., 7, 5937–5943, https://doi.org/10.5194/acp-7-5937-2007, 2007.

Boucher, O., Randall, D., Artaxo, P., Bretherton, C., Feingold, G., Forster, P., Kerminen, V.-M., Kondo, Y., Liao, H., Lohmann, U., Rasch, P., Satheesh, S., Sherwood, S., Stevens, B., and Zhang, X.: Clouds and Aerosols, in: Climate Change 2013: The Physical Science Basis. Contribution of Working Group I to the Fifth Assessment Report of the Intergovernmental Panel on Climate Change, edited by Stocker, T.F., Qin, D., Plattner, G.-K., Tignor, M., Allen, S., Boschung, J., Nauels, A., Xia, Y., Bex, V., and Midgley, P., Cambridge Univ. Press, Cambridge, UK and New York, NY, USA, 2013.

Bovensmann, H., Burrows, J. P., Buchwitz, M., Frerick, J., Noël, S., Rozanov, V. V., Chance, K. V., and Goede, A. P. H.: SCIAMACHY: Mission Objectives and Measurement Modes, J. Atmos. Sci., 56, 127–150, https://doi.org/10.1175/1520-0469, 1999.

Chand, D., Anderson, T. L., Wood, R., Charlson, R. J., Hu, Y., Liu, Z., and Vaughan, M.: Quantifying above-cloud aerosol using spaceborne lidar for improved understanding of cloud-sky direct climate forcing, J. Geophys. Res., 113, D13206, https://doi.org/10.1029/2007JD009433, 2008.

Chand, D., Wood, R., Anderson, T. L., Satheesh, S. K., and Charlson, R. J.: Satellite-derived direct radiative effect of aerosols dependent on cloud cover, Nat. Geosci., 2, https://doi.org/10.1038/NGEO437, 2009.

Coddington, O. M., Pilewskie, P., Redemann, J., Platnick, S., Russell, P. B., Schmidt, K. S., Gore, W. J., Livingston, J., Wind, G., and Vukicevic, T.: Examining the impact of overlying aerosols on the retrieval of cloud optical properties from passive remote sensing, J. Geophys. Res., 115, D10211, https://doi.org/10.1029/2009JD012829, 2010.

Cox, C. and Munk, W.: Measurement of the Roughness of the Sea Surface from Photographs of the Sun's Glitter, J. Opt. Soc. Am., 44, 838–850, https://doi.org/10.1364/JOSA.44.000838, http://www.osapublishing.org/abstract.cfm?URI=josa-44-11-838, 1954.

de Graaf, M., Stammes, P., Torres, O., and Koelemeijer, R. B. A.: Absorbing Aerosol Index: Sensitivity Analysis, application to GOME and comparison with TOMS, J. Geophys. Res., 110, D01201, https://doi.org/10.1029/2004JD005178, 2005.

de Graaf, M., Stammes, P., and Aben, E. A. A.: Analysis of reflectance spectra of UV-absorbing aerosol scenes measured by SCIAMACHY, J. Geophys. Res., 112, D02206, https://doi.org/10.1029/2006JD007249, 2007.

de Graaf, M., Tilstra, L. G., Wang, P., and Stammes, P.: Retrieval of the aerosol direct radiative effect over clouds from spaceborne spectrometry, J. Geophys. Res., 117, https://doi.org/10.1029/2011JD017160, 2012.

de Graaf, M., Bellouin, N., Tilstra, L. G., Haywood, J., and Stammes, P.: Aerosol direct radiative effect of smoke over clouds over the southeast Atlantic Ocean from 2006 to 2009, Geophys. Res. Lett., https://doi.org/10.1002/2014GL061103, http://dx.doi.org/10.1002/2014GL061103, 2014.

de Graaf, M., Sihler, H., Tilstra, L. G., and Stammes, P.: How big is an OMI pixel?, Atmos. Meas. Tech., https://doi.org/10.5194/amt-9-3607-2016, http://www.atmos-meas-tech.net/9/3607/2016/, 2016.

de Graaf, M., Tilstra, L., and Stammes, P.: Aerosol direct radiative effect over clouds from synergic OMI and MODIS reflectance, Atmos. Meas. Tech. Disc., 19, xx – xx, 2019.

Deaconu, L. T., Waquet, F., Josset, D., Ferlay, N., Peers, F., Thieuleux, F., Ducos, F., Pascal, N., Tanré, D., Pelon, J., and Goloub, P.: Consistency of aerosols above clouds characterization from A-Train active and passive measurements, Atmos. Meas. Tech., 10, 3499–3523, https://doi.org/10.5194/amt-10-3499-2017, 2017.

Deschamps, P. Y., Breon, F. M., Leroy, M., Podaire, A., Bricaud, A., Buriez, J. C., and Seze, G.: The POLDER mission: instrument characteristics and scientific objectives, IEEE Transactions on Geoscience and Remote Sensing, 32, 598–615, https://doi.org/10.1109/36.297978, 1994.

Feng, N. and Christopher, S. A.: Measurement-based estimates of direct radiative effects of absorbing aerosols above clouds, J. Geophys. Res., 120, 6908–6921, https://doi.org/10.1002/2015JD023252, 2015.

Forster, P., Ramaswamy, V., Artaxo, P., Berntsen, T., Betts, R., Fahey, D. W., Haywood, J., Lean, J., Lowe, D. C., Myhre, G., Nganga, J., Prinn, R., Raga, G., Schulz, M., and Van Dorland, R.: Contribution of Working Group I to the Fourth Assessment Report of the Intergovernmental Panel on Climate Change, in: Climate Change 2007: The Physical Science Basis., edited by Solomon, S., Qin, D., Manning, M., Chen, Z., Marquis, M., Averyt, K., Tignor, M., and Miller, H., p. 996, Cambridge Univ. Press, Cambridge, UK and New York, NY, USA, 2007.

Haywood, J. M., Osborne, S. R., and Abel, S. J.: The effect of overlying absorbing aerosol layers on remote sensing retrievals of cloud effective radius and cloud optical depth, Q. J. R. Meteorol. Soc., 130, 779–800, https://doi.org/10.1256/qj.03.100, 2004.

Jethva, H. and Torres, O.: Satellite-based evidence of wavelength-dependent aerosol absorption in biomass burning smoke inferred from Ozone Monitoring Instrument, Atmos. Chem. Phys., 11, 10 541–10 551, https://doi.org/10.5194/acp-11-10541-2011, 2011.

Jethva, H., Torres, O., Remer, L. A., and Bhartia, P. K.: A Color Ratio Method for Simultaneous Retrieval of Aerosol and Cloud Optical Thickness of Above-Cloud Absorbing Aerosols From Passive Sensors: Application to MODIS Measurements, IEEE T. Geosci. Remote, 51, 3862–3870, https://doi.org/10.1109/TGRS.2012.2230008, 2013.

Jethva, H., Torres, O., Waquet, F., Chand, D., and Hu, Y.: How do A-train Sensors Intercompare in the Retrieval of Above-Cloud Aerosol Optical Depth? A Case Study-based Assessment, Geophys. Res. Lett., 41, https://doi.org/10.1002/2013GL058405, 2014.

Levelt, P. F., van den Oord, G. H. J., Dobber, M. R., Mälkki, A., Visser, H., de Vries, J., Stammes, P., Lundell, J. O. V., and Saari, H.: The ozone monitoring instrument, IEEE T. Geosci. Remote, 44, 1093–1101, 2006.

Marbach, T., Riedi, J., Lacan, A., and Schluessel, P.: The 3MI Mission: Multi-Viewing -Channel -Polarisation Imager of the EUMETSAT Polar System -Second Generation (EPS-SG) dedicated to aerosol and cloud monitoring, Proc SPIE, 9613, 10–1, https://doi.org/10.1117/12.2186978, 2015.

Meyer, K., Platnick, S., Oreopoulos, L., and Lee, D.: Estimating the direct radiative effect of absorbing aerosols overlying marine boundary layer clouds in the southeast Atlantic using MODIS and CALIOP, J. Geophys. Res., 118, https://doi.org/10.1002/jgrd.50449, 2013.

Meyer, K., Platnick, S., and Zhang, Z.: Simultaneously inferring above-cloud absorbing aerosol optical thickness and underlying liquid phase cloud optical and microphysical properties using MODIS, J. Geophys. Res., 120, 5524–5547, https://doi.org/10.1002/2015JD023128, 2015.

Myhre, G., Samset, B. H., Schulz, M., Balkanski, Y., Bauer, S., Berntsen, T. K., Bian, H., Bellouin, N., Chin, M., Diehl, T., Easter, R. C., Feichter, J., Ghan, S. J., Hauglustaine, D., Iversen, T., Kinne, S., Kirkevåg, A., Lamarque, J.-F., Lin, G., Liu, X., Lund, M. T., Luo, G., Ma, X., van Noije, T., Penner, J. E., Rasch, P. J., Ruiz, A., Seland, Ø., Skeie, R. B., Stier, P., Takemura, T., Tsigaridis, K., Wang, P., Wang, Z., Xu, L., Yu, H., Yu, F., Yoon, J.-H., Zhang, K., Zhang, H., and Zhou, C.: Radiative forcing of the direct aerosol effect from AeroCom Phase II simulations, Atmos. Chem. Phys., 13, 1853–1877, https://doi.org/10.5194/acp-13-1853-2013, 2013.

Peers, F., Waquet, F., Cornet, C., Dubuisson, P., Ducos, F., Goloub, P., Szczap, F., Tanré, D., and Thieuleux, F.: Absorption of aerosols above clouds from POLDER/PARASOL measurements and estimation of their direct radiative effects, Atmos. Chem. Phys., 15, 4179–4196, https://doi.org/10.5194/acp-15-4179-2015, 2015.

Russell, P. B., Bergstrom, R. W., Shinozuka, Y., Clarke, A. D., DeCarlo, P. F., Jimenez, J. L., Livingston, J. M., Redemann, J., Dubovik,
5   O., and Strawa, A.: Absorption Angstrom Exponent in AERONET and related data as an indicator of aerosol composition, Atmos. Chem. Phys., 10, 1155–1169, https://doi.org/10.5194/acp-10-1155-2010, 2010.

Schulte, R.: A quantitative comparison of spaceborne spectrometry and polarimetry measurements of the aerosol direct radiative effect over clouds, Tech. Rep. KNMI IR–2016–09, Royal Netherlands Meteorological Institute (KNMI), 2016.

Torres, O., Jethva, H., and Bhartia, P. K.: Retrieval of Aerosol Optical Depth above Clouds from OMI Observations: Sensitivity Analysis and
10   Case Studies, J. Atmos. Sci., 69, 0022–4928, https://doi.org/10.1175/JAS-D-11-0130.1, 2011.

van der Werf, G. R., Randerson, J. T., Giglio, L., Collatz, G. J., Mu, M., Kasibhatla, P. S., Morton, D. C., DeFries, R. S., Jin, Y., and van Leeuwen, T. T.: Global fire emissions and the contribution of deforestation, savanna, forest, agricultural, and peat fires (1997–2009), Atmos. Chem. Phys., 10, 11 707–11 735, https://doi.org/10.5194/acp-10-11707-2010, 2010.

Wang, P., Stammes, P., van der A, R., Pinardi, G., and van Roozendael, M.: FRESCO+: an improved O_2 A-band cloud retrieval algorithm
15   for tropospheric trace gas retrievals, Atmos. Chem. Phys., 8, 6565–6576, https://doi.org/10.5194/acp-8-6565-2008, 2008.

Waquet, F., Cornet, C., Deuzé, J.-L., Dubovik, O., Ducos, F., Goloub, P., Herman, M., Lapyonok, T., Labonnote, L. C., Riedi, J., Tanré, D., Thieuleux, F., and Vanbauce, C.: Retrieval of aerosol microphysical and optical properties above liquid clouds from POLDER/PARASOL polarization measurements, Atmos. Meas. Tech., 4, 991–1016, https://doi.org/10.5194/amt-6-991-2013, 2013a.

Waquet, F., Peers, F., Ducos, F., Goloub, P., Platnick, S., Riedi, J., Tanré, D., and Thieuleux, F.: Global analysis of aerosol properties above
20   clouds, Geophys. Res. Lett., 40, 5809–5814, https://doi.org/10.1002/2013GL057482, 2013b.

Wilcox, E. M.: Direct and semi-direct radiative forcing of smoke aerosols over clouds, Atmos. Chem. Phys., 12, 139–149, https://doi.org/10.5194/acp-12-139-2012, 2012.

Yu, H. and Zhang, Z.: New Directions: Emerging satellite observations of above-cloud aerosols and direct radiative forcing, Atmos. Environ., 72, 36–40, https://doi.org/http://dx.doi.org/10.1016/j.atmosenv.2013.02.017, 2013.

25 Zeng, S., Cornet, C., Parol, F., Riedi, J., and Thieuleux, F.: A better understanding of cloud optical thickness derived from the passive sensors MODIS/AQUA and POLDER/PARASOL in the A-Train constellation, Atmos. Chem. Phys., 12, 11 245–11 259, https://doi.org/10.5194/acp-12-11245-2012, 2012.

Zhang, Z., Meyer, K., Platnick, S., Oreopoulos, L., Lee, D., and Yu, H.: A novel method for estimating shortwave direct radiative effect of above-cloud aerosols using CALIOP and MODIS data, Atmos. Meas. Tech., 7, 1777–1789, https://doi.org/10.5194/amt-7-1777-2014,
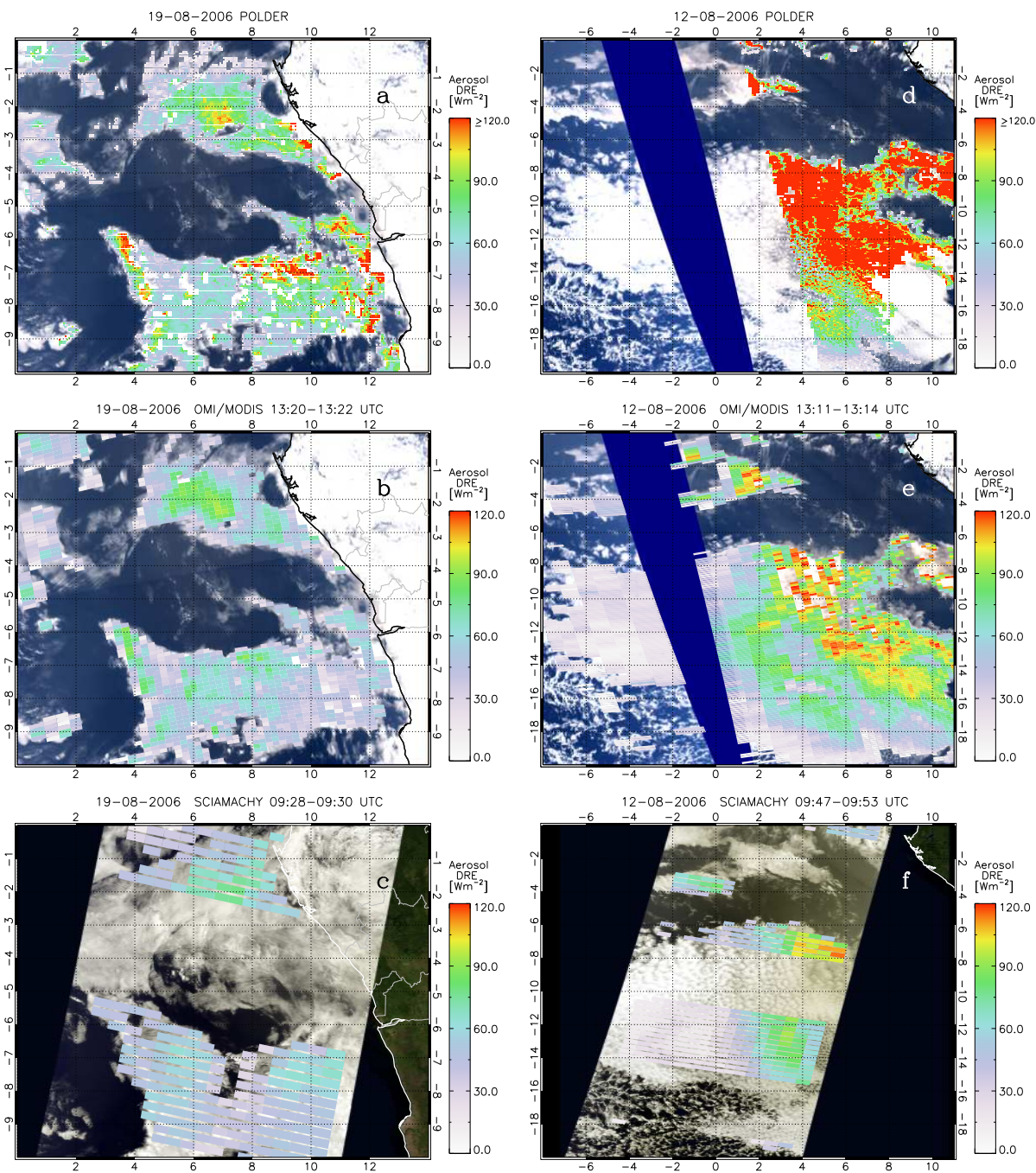30   2014.

Figure 1. (a) Instantaneous Aerosol Direct Radiative Effect (DRE) over clouds on 19 August 2006 from POLDER, overlaid over a MODIS RGB image; (b) Aerosol DRE over clouds on the same day from a combination of OMI and MODIS reflectances, overlaid over the same MODIS RGB image; (c) Aerosol DRE over clouds from SCIAMACHY on the same day, overlaid over a MERIS RGB image; (d–f) same as (a–c) for 12 August 2006. The areas are centered over the MERIS/SCIAMACHY overpasses.
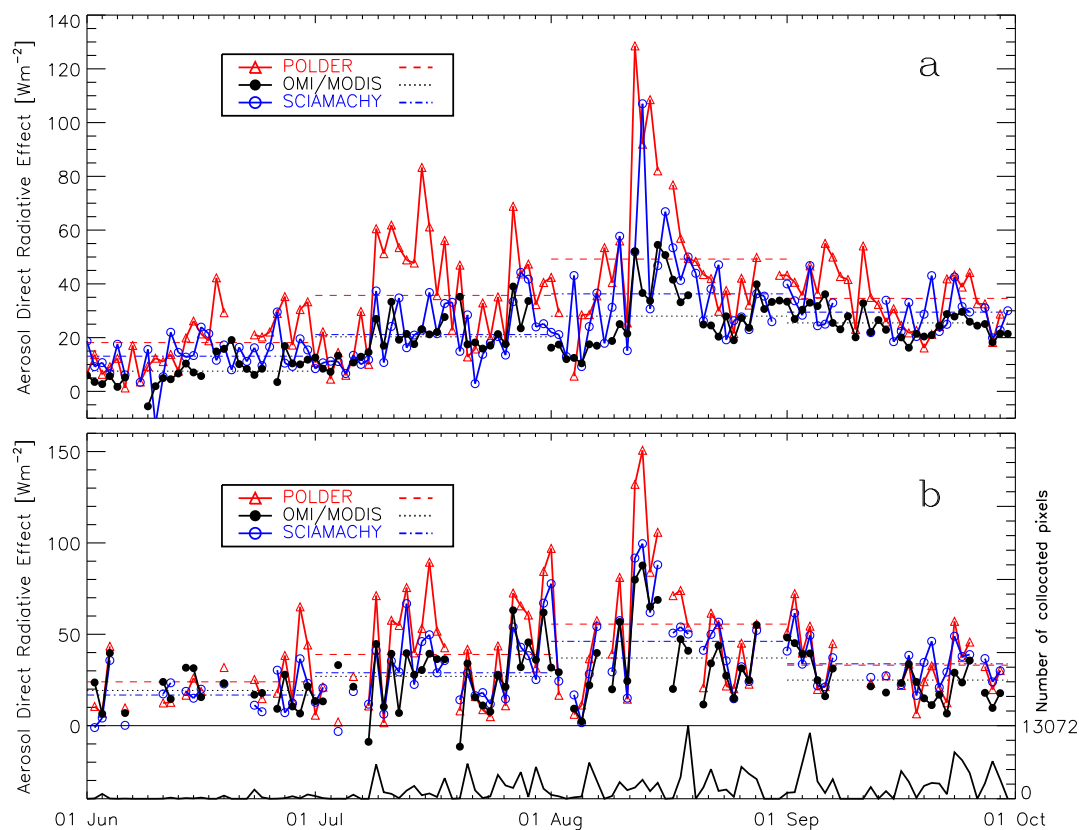
Figure 2. a) Noon-normalized instantaneous aerosol DRE over clouds from combined OMI/MODIS reflectances (black), SCIAMACHY reflectances (blue) and POLDER AOT and COT retrievals (red) from 1 June - 1 October 2006, averaged over the area 10°N–20°S;10°W–20°E in the south-east Atlantic. The average monthly aerosol DRE over clouds are given by the coloured straight lines during each month. b) Same as a), but for collocated POLDER, regridded OMI/MODIS and regridded SCIAMACHY pixels only. The number of collocated pixels that are covered by all three instruments is given in the lower panel in b).
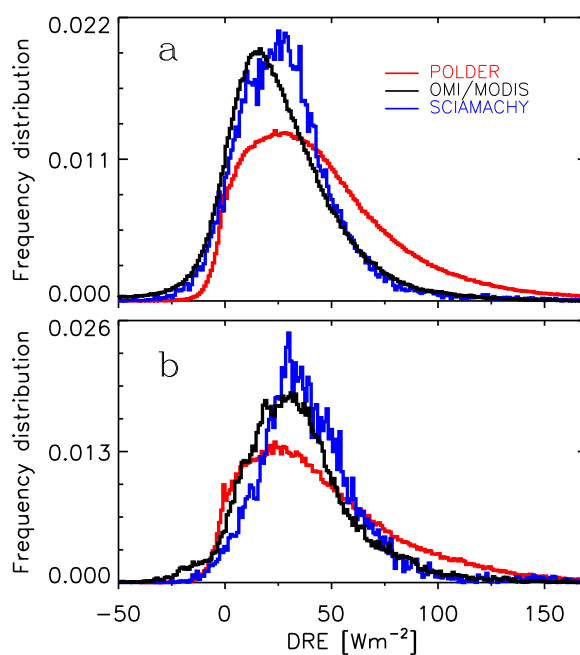
Figure 3. a) Histograms of aerosol DRE over clouds in the Atlantic Ocean during June – September 2006 from combined OMI/MODIS reflectance spectra (black), SCIAMACHY reflectance spectra (blue) and POLDER AOT and COT retrievals (red). b) Same as a) but for collocated POLDER, regridded OMI/MODIS and regridded SCIAMACHY pixels only.
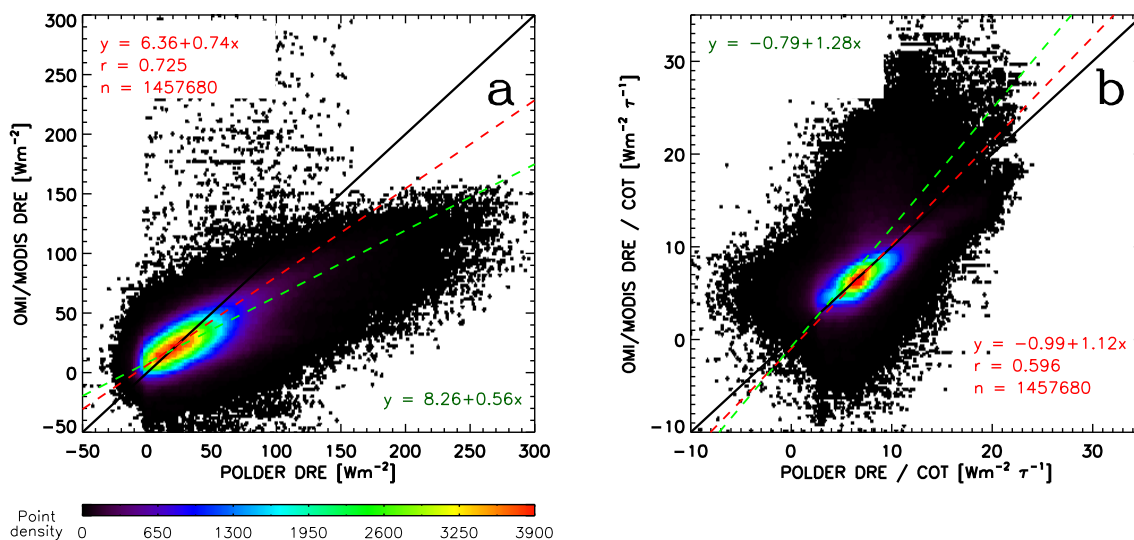
Figure 4. (a) Scatterplot of POLDER DRE versus DRE from regridded OMI/MODIS data. The green dashed line shows an unweighted linear least-squares fit, the red dashed line shows a linear least-squares fit weighted to the majority of the points in the center. (a) same as (b), but for the quantity DRE/COT.
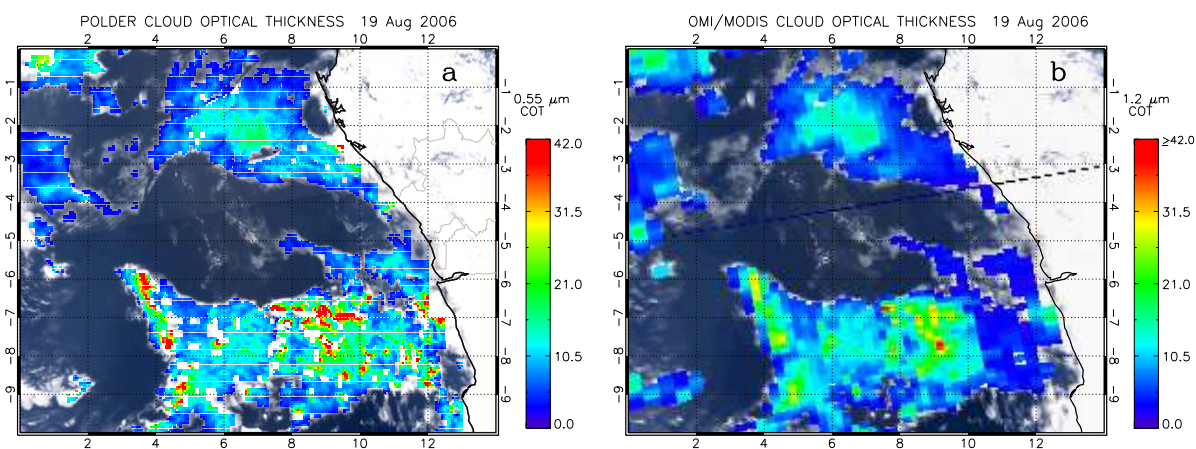

Figure 5. Cloud optical thickness (COT) overplotted on a MODIS RGB image on 19 August 2006 for (a) POLDER at 550 nm and (b) OMI/MODIS at 1.2 micron, regridded to 6×6 km^2 grid boxes.